A Generic Centerline Velocity Decay Curve for Initially Turbulent Axisymmetric Jets[1]

George Papadopoulos[2]

William M. Pitts

Building and Fire Research Laboratory,
National Institute of Standards
and Technology,
Gaithersburg, MD 20899

Recently the authors introduced a length scale which effectively collapsed the near field centerline development of velocity and mass fraction for variable density axisymmetric jets whose initial conditions correspond to those of fully developed turbulent pipe flow. The new length scale incorporated the initial mass, momentum, and turbulence intensity per unit area to capture the Reynolds number dependence of near field development for the velocity and scalar distributions observed in low Reynolds number turbulent jets. The present paper extends the analysis for a constant density jet to the intermediate and self-similar far fields further downstream using a dynamic length scale based on the local centerline turbulence intensity. The normalized mean velocity distributions of an air jet collapse over the entire flow distance investigated when the axial distance is normalized by the proposed length scale, thus scaling the virtual origin shift and effectively incorporating the Reynolds number dependence.

1 Introduction

Axisymmetric turbulent jets are used in a variety of engineering applications because of their ability to provide high mixing rates in simple and safe configurations. To better control such mixing processes accurate prediction of jet dynamics is necessary, especially in the early stages of development where important interacting processes, such as, combustion, recirculation, and entrainment, are initiated.

There is a considerable volume of information on jets available in the literature (Harsha, 1971; Chen and Rodi, 1980; Gouldin et al., 1986) and it is safe to say that a good understanding exists on jet characteristics and development in the far-field, or self-similar region. In this region of flow the mean and fluctuating centerline distribution field of a constant density axisymmetric jet issuing into a still ambient is described by the following equations:

$$\frac{\bar{U}(0,0)}{\bar{U}(z,0)} = K_u\left(\frac{z - z_{o,u}}{r_\epsilon}\right),$$

$$\frac{U'(z,0)}{\bar{U}(z,0)} = \text{constant} \qquad (1)$$

K_u is the centerline decay rate for the velocity distribution, $U(z, r)$. The streamwise distance, z, is measured from the jet exit plane, but to achieve a generic set of equations the introduction of a virtual origin, z_o, is necessary. This latter term is a displacement along the centerline of the jet representing a correction to the actual origin that yields the location where an idealized point jet-source, having the same mass, momentum and far-field development as the actual jet, would be located. It can thus be regarded as a means of incorporating the effects of nonideal initial conditions and flow development.

The effective radius,

$$r_\epsilon = \frac{\dot{m}_o}{(\pi\rho_\infty J_o)^{1/2}}, \qquad (2)$$

introduced in a simpler form first by Thring and Newby (1953) and used in this form by several researchers (Dahm and Dimotakis, 1987; Dowling and Dimotakis, 1990; Pitts, 1991a; Richards and Pitts, 1993) incorporates some initial conditions, such as density ratio $R_\rho = \rho_o/\rho_\infty$ and velocity distribution nonuniformity, through the mass and momentum fluxes at the jet exit plane, $\dot{m}_o$ and J_o, respectively. Dahm and Dimotakis (1990) have shown, using dimensional analysis, that the effective radius as defined in Eq. (2) is the appropriate length scale to nondimensionalize the axial coordinate of the jet fluid concentration in the far-field. After a detailed study of variable density jets, Richards and Pitts (1993) concluded that the final asymptotic state of all momentum-dominated axisymmetric jets depends only on the rate of momentum addition when the streamwise distance is scaled appropriately with r_ϵ. They furthermore showed, regardless of the initial conditions (fully developed pipe and nozzle flow), axisymmetric turbulent free jets decay at the same rate, spread at the same half-angle, and both the mean and rms mass fraction values collapse in a form consistent with full self-preservation. Nevertheless, the problem of the virtual origin still remained, and represented an unknown parameter that needed to be determined specifically for each configuration.

Investigations focusing on the variation of the virtual origin have indicated qualitatively how various initial parameters, such as Reynolds number, profile shape, turbulence intensity, and density ratio, affect its location. Some attempts at quantifying the trends observed, especially with respect to Reynolds number, have yielded empirical relations that are merely best fits to specific experimental data (see discussion by Pitts, 1991b). These correlations indicate a downstream displacement of z_o with increasing Re, reaching an asymptotic value at large Re.

In a recent investigative effort undertaken by the authors (Papadopoulos and Pitts, 1998) the controlling parameter responsible for the variation of centerline velocity and concentration decay characteristics in the near field of jets whose exit characteristics correspond to those of fully developed turbulent pipe flow was identified to be the initial turbulence intensity per unit area. The initial turbulence intensity is a significant source of excitation that feeds into the growing shear layer, thus governing directly the growth of turbulence responsible

[1] Contribution of the National Institute of Standards and Technology and not subject to copyright in the United States.

[2] Current address: Dantec Measurement Technology, Inc., 777 Corporate Drive, Mahwah, NJ 07430.

Contributed by the Fluids Engineering Division for publication in the JOURNAL OF FLUIDS ENGINEERING. Manuscript received by the Fluids Engineering Division March 23, 1996; revised manuscript received November 25, 1998. Associate Technical Editor: F. Hussain.

for breaking up the jet potential core and for transitioning the jet into a fully developed self-similar flow. Combining the initial turbulence intensity per unit area with the definition of the effective radius resulted in a new length scale that captured the near field variation of velocity and scalar centerline decay with Re, and thus collapsed the distributions for these types of turbulent axisymmetric jets. However, the proposed axial scaling was inappropriate when extended to the intermediate and far fields of the jet.

In related work, Faeth and coworkers (Wu et al., 1992; Wu and Faeth, 1993; Wu et al., 1995) investigated the breakup of liquid jets flowing into gas surroundings. Similar to our findings, the degree of jet breakup was shown to depend on the initial turbulence level of the liquid jet. However, the physical processes responsible for the breakup of liquid jets are very different from that proposed for the variation of the initial development rate of a gas jet with initial turbulence intensity level.

The present paper focuses on the centerline velocity field of a constant density jet and extends the aforementioned work by presenting a similar length scale that is more robust, in that not only does it collapse the near-field centerline behavior for variable Re cases, but also the intermediate and far fields as well. Furthermore, it yields a generic centerline mean velocity curve with a single value for the virtual origin. This unique generic curve can be used to predict the velocity virtual origin and centerline development for all axisymmetric jets having fully developed turbulent pipe flow initial conditions.

2 Experimental Setup and Apparatus

Test Configuration. Measurements were performed in a jet produced by a long straight pipe having a sharp-edged exit. The diameter was 6.08 mm ± 0.04 mm.[3] The gas supply to the pipe passed first into a cylindrical settling chamber (120 mm long and 100 mm in diameter) and then through a series of pipe fittings before entering the pipe. The fittings provided the necessary initial artificial disturbance to guarantee fully developed turbulent conditions at the exit of the pipe, 103 diameters downstream, for the flow rates considered in the investigation.

Air was the working fluid supplied from an in-house pressurized distribution system. It was filtered to remove oil, moisture, and particulates. A long supply line with several looped copper sections ensured that the issuing gas was in temperature equilibrium with the ambient air. A 100 L/min mass flow controller, accurate to ±1 percent of full scale and with repeatability of ±0.2 percent of full scale per manufacturer's specifications, was used to meter the gas. Calibration of the mass flow controller was performed using an Optiflow 730 Digital Flowmeter.[4] The uncertainty in the mass flow calibration was less than ±1.5 percent. Ambient conditions, temperature and barometric pressure, were recorded at the beginning and end of each complete test (generally lasting 2 h to 3 h) for determining the average gas properties. Overall, beginning-to-end ambient variations were small, less than ±0.5°C and ±2 Pa. The resulting uncertainty in the bulk flow velocity based on the mass flow controller setting was ±2 percent, which yielded an uncertainty in Re of ±2.2 percent.

Velocity Measurements. A single wire, hot-wire probe was used to measure the velocity at the exit of the pipe and along the centerline of the air jet. The probe was a 2.5-μm-diameter tungsten wire with a sensing length of 0.4 mm. It was controlled by a TSI IFA100 anemometer, interfaced to a Masscomp computer, which incorporated voltage gain and offset capabilities for optimizing the analog output for the voltage range of the 12-bit analog-to-digital converter. Calibration of the hot-wire was performed using a TSI Model 1125 calibrator unit over a velocity range of 2 m/s to 60 m/s. The calibration data was fitted to a general King's law relation, $E^2 = A + BU^n$, where E is the hot-wire voltage output, and A, B, n are calibration constants. The absolute error in an individual velocity measurement was estimated to be no more than 4 percent. The square wave frequency response of the hot-wire was approximately 25 kHz. Data sampling was performed at 500 Hz and 10 kHz, 10,000 and 30,000 samples, respectively, with the high sampling rate used to better evaluate velocity dynamics in the near and intermediate fields ($0 \leq z/r_o \leq 21$). The uncertainties associated with determining the mean and rms values were less than 0.2 percent of the initial centerline mean velocity at the exit of the jet.

The pipe assembly was fixed horizontally on a lab bench with the jet issuing into the laboratory. Fine meshed screens placed at a standoff distance of about 0.3 m surrounded the jet to limit the effects of cross-currents in the room. A two-dimensional computer-controlled traverse was used to move the hot-wire probe in relation to the jet. For measuring the exit velocity distribution, the wire was centered longitudinally along

[3] Reported expanded uncertainties are at 95 percent confidence (2σ).

[4] Certain commercial equipment, instruments or materials are identified in this paper in order to adequately specify the experimental procedure. Such identification does not imply recommendation or endorsement by the National Institute of Standards and Technology, nor does it imply that the materials or equipment are necessarily the best available for the purpose.

Nomenclature

A = jet cross-sectional area
J_o = initial momentum flux ($= \int_A \rho U(0, r)^2 dA$)
K = centerline decay rate
$\dot{m}_o$ = initial mass flux ($= \int_A \rho U(0, r) dA$)
M_o = initial volume flux for constant density jet ($= \int_A U(0, r) dA$)
N_o = initial momentum flux normalized by density for constant density jet ($= \int_A U(0, r)^2 dA$)
r_o = initial jet radius
r_u = contribution to r_ϵ due to mean velocity profile at jet exit
r_ϵ = effective jet radius
r^* = length scale incorporating mass, momentum and turbulence intensity characteristics
R_ρ = density ratio ($= \rho_o/\rho_\infty$)
Re = Reynolds number ($= 2r_o U_b \rho_o/\mu_o$)
t = time
Tu = turbulence intensity ($= U'/\bar{U}$)
U = velocity
z = streamwise distance, measured from jet exit and positive in bulk flow direction
z_o = virtual origin
η = normalized centerline turbulence intensity
μ = dynamic viscosity
ρ = density
τ_o = initial turbulence intensity per unit area ($= 1/A \int_A Tu(0, r) dA$)

Subscripts and Other Notation

o = an initial condition
0.5 = streamwise location where the centerline velocity equals half of the maximum jet velocity at the exit
∞ = ambient (surroundings)
b = bulk (average)
l = local field
m = maximum
pc = potential core end location
u = velocity field
$( )'$ = denotes root mean squared (rms) value
$\overline{( )}$ = denotes time averaged mean value

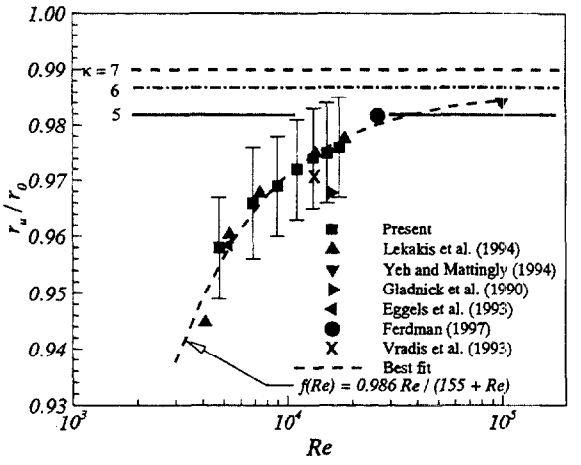

Fig. 1 Normalized effective radii due to the exit velocity distribution dependence on Re

a jet diameter and traversed perpendicular to it with the wire's longitudinal axis normal to the travel and incoming flow directions. The streamwise location of this measurement was z = 0.5 mm. Centerline measurements were performed up to a location of z = 270 mm. The error in initially positioning the probe was less than ±0.05 mm and ±0.1 mm in the radial and streamwise directions, respectively. Subsequent positioning was done at manufacturer's specified accuracy of ±1.6 μm and ±3.2 μm, respectively.

3 Results

Mass, momentum, and turbulence intensity distributions at the exit plane influence flow development in the near field of the jet, the latter being a perturbation mechanism that feeds into the growing shear layer. Initial mass and momentum distributions are already incorporated in the definition of the effective radius, Eq. (2). Since the gas density is constant across the exit of the jet, Eq. (2) may be written as

$$r_\epsilon = r_u; \quad r_u = \frac{M_o}{(\pi N_o)^{1/2}} \tag{3}$$

where $M_o = \int_A U(0, r)dA$ and $N_o = \int_A U(0, r)^2 dA$. The term r_u is the contribution to the effective radius of the mean velocity profile at the exit. For a uniform (top-hat) profile $r_u = r_o$, while for a parabolic profile $r_u = \sqrt{3}r_o/2$. For a turbulent velocity profile r_u is determined by integrating the profile at the pipe exit. Doing so for the present data, as well as for other data found in the literature, gives the results shown in Fig. 1. The horizontal lines in the figure show the expected values if the typical power law profile is assumed,

$$\frac{\bar{U}(0, r)}{\bar{U}(0, 0)} = \left(1 - \frac{r}{r_o}\right)^{1/\kappa}, \tag{4}$$

where κ takes on values from 5 to 7 as Re increases within the range of the experimental data shown (Schlichting, 1979). An obvious difference of a few percent exists between the power law profile and actual experimental measurements for Re < 10,000.

In the authors' previous work (Papadopoulos and Pitts, 1998) a new length scale was defined,

$$r_o^* = r_\epsilon \tau_o^{-1/2} = \frac{R_\rho^{1/2} M_o}{(\pi N_o \tau_o)^{1/2}} \tag{5}$$

which incorporated the jet's initial mass, momentum, and turbulence intensity, the latter through the turbulence intensity per unit area, τ_o, shown in Fig. 2. Correcting for nonuniform velocity distribution effects had previously involved only the mean characteristics. For turbulent flows, however, the inclusion of fluctuating velocity effects in the definition of a scale was clearly necessary to fully capture the effects of initial conditions on flow development. If the velocity terms in the mass and momentum flux terms of Eq. (3) are separated into mean and fluctuating components, and subsequently time averaged, then an additional term multiplying the mean momentum flux term is apparent. This term is a function of the local turbulence intensity, and although not exactly equivalent to τ_o, it supports the general form of Eq. (5). Normalization of the streamwise distance by r_o^* was shown in this prior investigation to collapse the near field centerline velocity and mass fraction decay curves over a range of Re.

The effectiveness of r_o^* on the present measurements and on those of others found in the literature is shown in Fig. 3 where the mean centerline velocity distribution for several Re is shown. However, since far field self-similarity requires that the flow be dependent only on the total mass and momentum flux, and not on any specific characteristics of the initial flow, the normalization by r_o^* naturally fails to correlate the data when extended to the far field region, as is evident in Fig. 4. Even so, it is an important contribution since it collapses the near field distributions without the introduction of any empirical constants.

To correct the aforementioned shortcoming of r_o^* it is clear that a dynamic term replacing the constant τ_o term is necessary. The effectiveness of r_o^* in the near field implies that this dynamic term be initially equal to τ_o. On the other hand, far field self-similarity requires that the effective radius be the proper length scale for nondimensionalizing the axial coordinate. Thus, in the far field the dynamic term needs to equal unity. These two bounds may be satisfied by introducing a dynamic term of the form $\tau_o^{-\eta/2}$ with $\eta = f(Tu)$ taking on values between one and zero, thus incorporating the expected decreasing effect of initial turbulence intensity on the growth of the shear layer as the jet propagates downstream.

A function for η meeting the aforementioned criteria may be defined in terms of the centerline turbulence intensity distribution, normalized to yield a value of one at the jet exit and zero in the far field. The result is

$$\eta = \frac{Tu(\infty, 0) - Tu(z, 0)}{Tu(\infty, 0) - Tu(0, 0)}, \tag{6}$$

where $Tu(\infty, 0)$ is the centerline turbulence intensity measured in the jet far field, which according to Eq. (1) is a constant throughout the self-similar region. Figure 5 shows distributions of η for several Re versus z/r_o^*, where

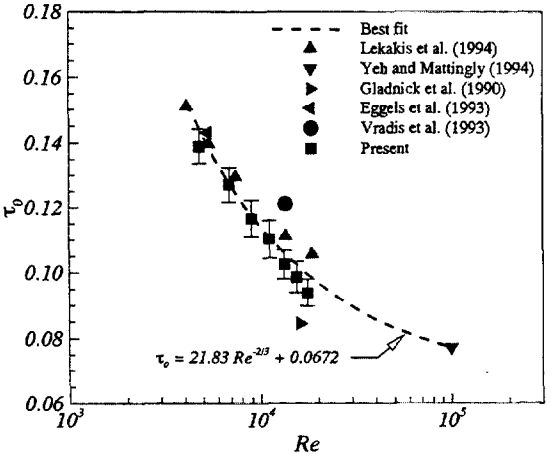

Fig. 2 Initial turbulence intensity per unit area as a function of Re

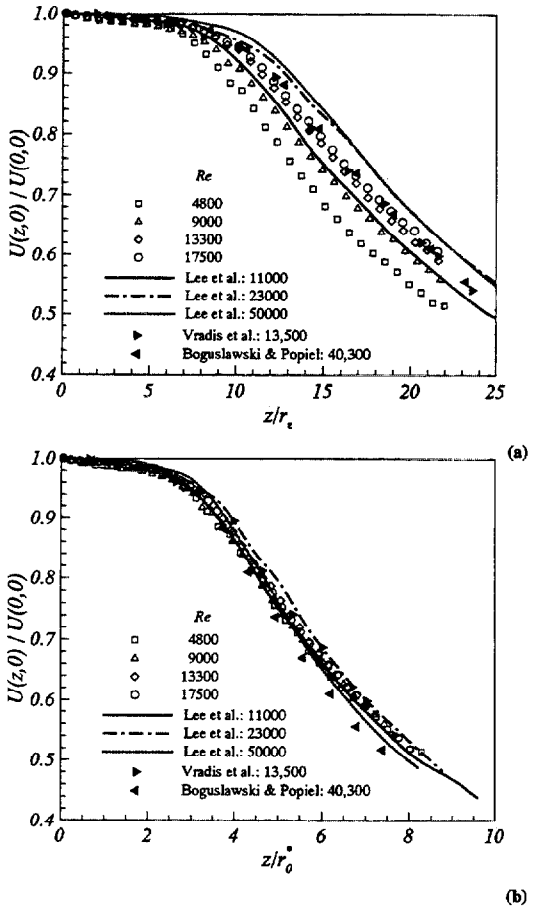

Fig. 3 Normalized mean centerline velocity decay for several Re: (*a*) axial distance normalized by effective radius; (*b*) axial distance normalized by a length scale based on initial mass momentum and turbulence intensity distributions

$$r_l^* = \tau_o^{-\eta/2} r_\epsilon \tag{7}$$

is the new dynamic length scale. Note that when $\eta = 0$ the flow becomes self-similar according to Eq. (1). Figure 5 then indicates that self-similarity is attained over shorter flow distances at lower Re, which agrees with earlier observations (Pitts, 1991b).

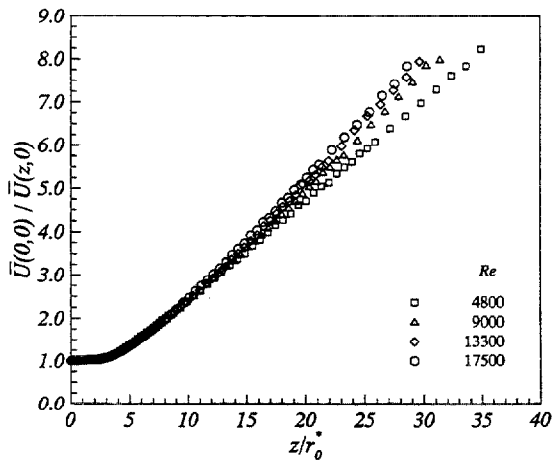

Fig. 4 Inverse decay of mean centerline velocity in near, intermediate and far fields of the air jet; axial distance normalized by r_o^*

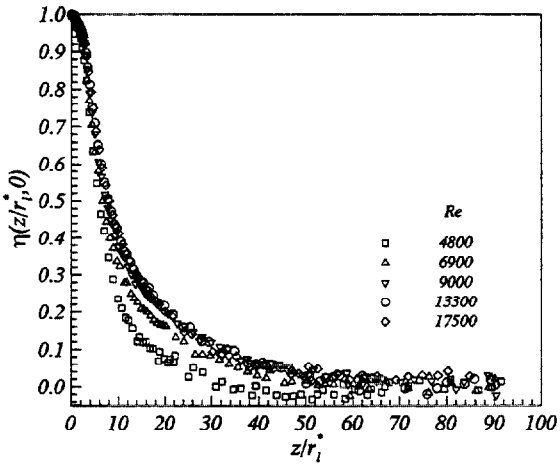

Fig. 5 Normalized centerline turbulence intensity distribution

Recasting the data of Fig. 4 in terms of z/r_l^* yields good results (Fig. 6), implying that a generic curve for the centerline velocity decay of initially turbulent axisymmetric jets can be realized when the streamwise distance variable is normalized using the newly proposed dynamic length scale. Such a generic realization also implies that a single value for the virtual origin exists for data normalized in this way. Its value is obtained by linearly fitting the far field velocity data of Fig. 6 ($z/r_l^* \geq 60$) and extrapolating to $\bar{U}(0, 0)/\bar{U}(z, 0) = 0$, as indicated by the dashed line. The result is $z_o/r_l^* = 6 \pm 1$.

Reverting back to absolute coordinates requires the use of Figs. 1, 2, and 5. By using the proposed dynamic scaling a generic centerline decay curve of the mean velocity is attained, but the second moment (turbulence intensity distribution) still exhibits Re dependence. Thus, it is necessary to construct empirical functions for $\eta(z/r_l^*, 0)$ using the data in Fig. 5. A function which fits the data well is

$$\eta(\zeta) = a_1 e^{-b_1 \zeta^{c_1}} + a_2 e^{-b_2 \zeta^{c_2}}:$$

$$\text{with } \zeta = z/r_l^* \quad \text{and} \quad a_1 + a_2 = 1 \tag{8}$$

where $a_{1,2}$, $b_{1,2}$, and $c_{1,2}$ are fit parameters that depend on Re. The resulting curves for $\eta(z/r_l^*, 0)$ are shown in Fig. 7. Figure 8 shows the variation of the constants with Re, in the range investigated. Note that only a_1 is shown in the figure since $a_2 = 1 - a_1$ by the constraint indicated in Eq. (8). Performing

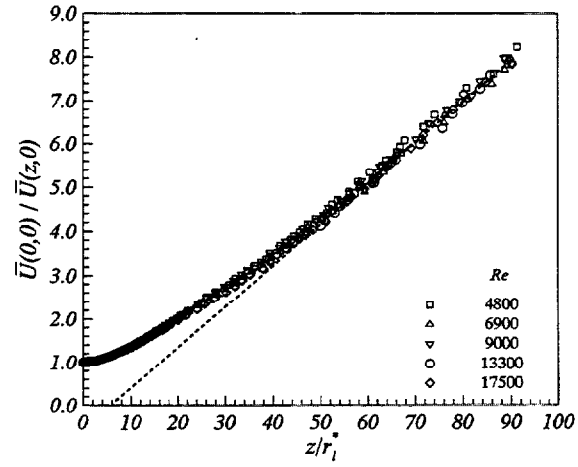

Fig. 6 Inverse decay of mean centerline velocity in near, intermediate and far fields of the air jet; axial distance normalized by the new dynamic length scale

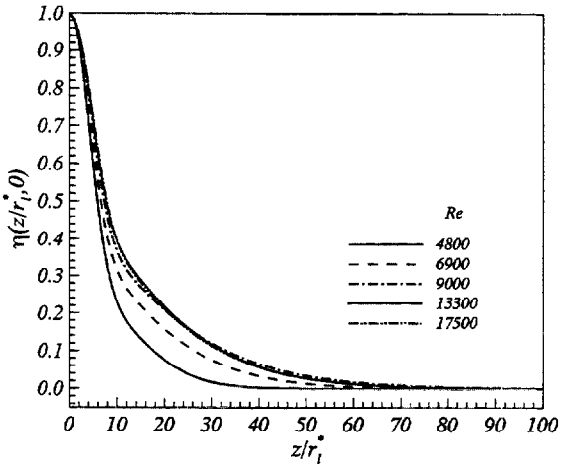

Fig. 7 Empirical curves for the normalized turbulence intensity distribution along the centerline of the jet

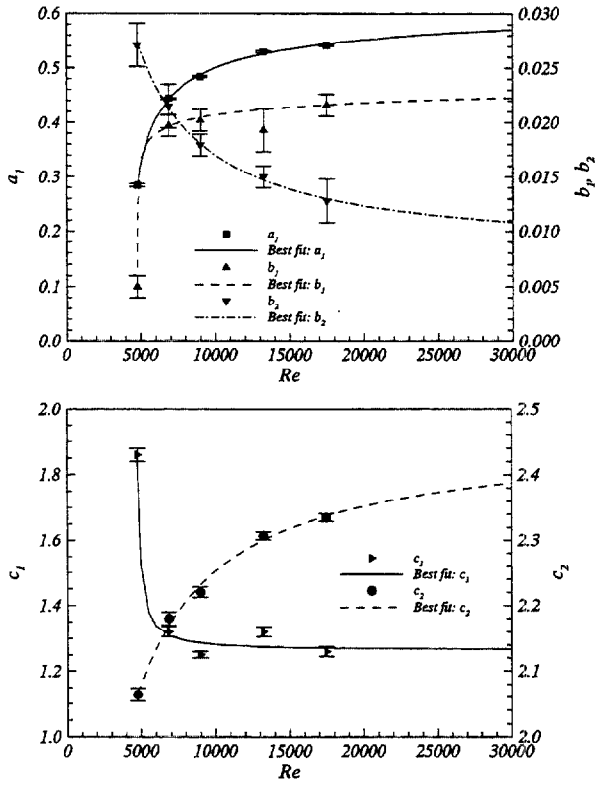

Fig. 8 Empirical fit parameters of Eq. (8) and their variation with Reynolds number

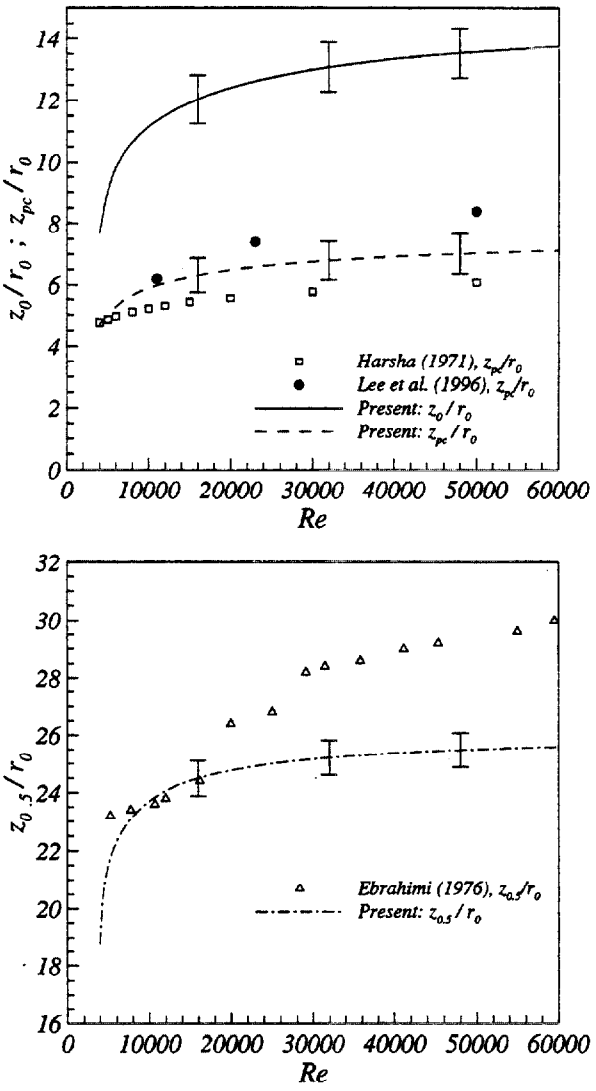

Fig. 9 Virtual origins, z_o, calculated using the generic velocity curve are shown as a function of Reynolds number in the upper panel. Calculated distances to the end of the potential core, z_{pc}, (upper panel) and the distance required for the centerline velocity to drop to half of its initial value, $z_{0.5}$, (lower panel) are also included and compared with appropriate literature measurements.

the necessary calculation for the virtual origin yields the absolute value of the origin, z_o/r_o, for each Reynolds number investigated in the present work, as seen in Fig. 9. Included in the figure are potential core measurements, z_{pc}/r_o, reported by Lee et al. (1996) and Harsha (1971), as well as the length to $\bar{U}(z, 0)/\bar{U}(0, 0) = 0.5$, $z_{0.5}/r_o$, reported by Ebrahimi (1976). These lengths are compared to similar lengths extracted from the generic curve. The agreement is good. It should be noted that the numbers reported by Harsha (1971) and Ebrahimi (1976) are for jets whose initial conditions are unclear and most likely (from their discussion) do not correspond to the type of jets reported here. Even so, the trend of the present data compares well, supporting the conclusions of the present investigation that the mean centerline velocity decay distribution for initially turbulent axisymmetric jets may be dynamically scaled to attain Reynolds number independence using r^*.

4 Conclusions

Centerline velocity data were presented for a constant density axisymmetric jet having a nonuniform initial velocity distribution that was fully turbulent. The several Reynolds numbers investigated showed distinctly the effect of Re on the development of the jet, specifically the downstream shift of the virtual origin with increasing Re. This shift of the centerline velocity decay curves was attributed to the initial turbulence intensity distribution, which may be thought of as a natural source of random excitation that disrupts vortex formation and pairing processes responsible for elevated momentum mixing under initial laminar conditions, and hence directly governs the changes in the growth of turbulence within the shear layer of the jet (Papadopoulos and Pitts, 1998). The relative magnitude of the initial turbulence intensity may be used to scale the changes in the growth of the shear layer and by forming an appropriate length scale render Re independence to the center-

line velocity decay distribution when the axial distance is normalized by this length scale. This was achieved in the near field by introducing a new length scale, r_o^*, that incorporated the initial mass, momentum and turbulence intensity distributions.

The effectiveness of r_o^* was, however, limited to the near field of the jet where the influence of initial conditions is greatest. As the jet develops, the effects of initial conditions rapidly diminish. In the self-similar region of the jet development becomes independent of initial conditions, and only the initial mass and momentum fluxes are important. Hence, to extend the near field scaling over the entire jet development region, this diminishing effect of initial conditions (turbulence intensity) was incorporated into the previously proposed near field length scale by using the local normalized centerline turbulence intensity field. The result was a dynamic length scale that effectively captured the virtual origin shift and collapsed the centerline mean velocity distribution curves for initially turbulent axisymmetric jets. From the generic curve a single value for the virtual origin location was obtained, this being $z_o/r_o^* = 6 \pm 1$.

The introduction of a local scale to capture the Reynolds number effect is similar to the approach of Sautet and Stepowski (1995 and 1996) who proposed replacing the ambient density with a local average density to better capture the effects of variable density on the near field decay of mass fraction in variable density jets. Although the present scaling has been shown to work for the velocity distribution of constant density jets, it should be feasible to extend it to the velocity and scalar distributions of variable density jets. Furthermore, by utilizing the idea of a local average density it may be possible to represent the mean dynamic and scalar centerline distributions of constant and variable density initially turbulent jets by a single generic curve. These last two points are presently being investigated.

References

Boguslawsk, L., and Popiel, Cz. O., 1979, "Flow Structure of the Free Round Turbulent Jet in the Initial Region," *Journal of Fluid Mechanics,* Vol. 90, pp. 531–539.

Chen, C. J., and Rodi, W., 1980, *Vertical Turbulent Buoyant Jets—A Review of Experimental Data,* Pergamon Press, New York.

Dahm, W. A., and Dimotakis, P. E., 1987, "Measurements of Entrainment and Mixing in Turbulent Jets," *AIAA Journal,* Vol. 25, pp. 1216–1223.

Dahm, W. A., and Dimotakis, P. E., 1990, "Mixing at Large Schmidt Number in the Self-Similar Far Field of Turbulent Jets," *Journal of Fluid Mechanics,* Vol. 217, pp. 299–330.

Dowling, D. R., and Dimotakis, P. E., 1990, "Similarity of the Concentration Field of Gas-Phase Turbulent Jets," *Journal of Fluid Mechanics,* Vol. 218, pp. 109–141.

Ebrahimi, I., 1976, "Axialer Verlauf der Geschwindigkeit in Luft-Freistrahlen," Forschung Ing.-Wes., Vol. 42, pp. 33–35.

Eggels, J. G. M., Westerweel, J., and Nieuwstadt, F. T. M., 1993, "Direct Numerical Simulation of Turbulent Pipe Flow," *Applied Science Research,* Vol. 51, pp. 319–324.

Ferdman, E., 1997, "An Experimental Investigation of the Initially Asymmetric Turbulent Jets," M.S. thesis, Polytechnic University, New York.

Gladnick, P. G., Enotiadis, A. C., LaRue, J. C., and Samuelsen, G. S., 1990, "Near-Field Characteristics of a Turbulent Coflowing Jet," *AIAA Journal,* Vol. 28, pp. 1405–1414.

Gouldin, F. C., Schefer, R. W., Johnson, S. C., and Kollmann, W., 1986, "Nonreacting Turbulent Mixing Flows," *Progress in Energy Combustion Science,* Vol. 12, pp. 257–303.

Harsha, P. T., 1971, "Free Turbulent Mixing: A Critical Evaluation of Theory and Experiment," *Arnold Engineering Development Center Report,* AED-TR-71-36.

Lee, D. H., Chung, Y. S., and Kim, D. S., 1996, "Surface Curvature Effects on Flow and Heat Transfer from a Round Impinging Jet," *31st ASME National Heat Transfer Conference,* HTD-Vol. 324, pp. 73–83.

Lekakis, I., Durst F., and Sender J., 1994, "LDA Measurements in the Near Wall Region of an Axisymmetric Sudden Expansion," *7th International Symposium on Applications of Laser Tecniques to Fluid Mechanics,* Lisbon, Portugal.

Papadopoulos, G., and Pitts, W. M., 1998, "Scaling the Near-Field Centerline Mixing Behavior of Axisymmetric Turbulent Jets," *AIAA Journal,* Vol. 36, pp. 1635–1642.

Pitts, W. M., 1991a, "Effects of Global Density Ratio on the Centerline Mixing Behavior of Axisymmetric Turbulent Jets," *Experiments in Fluids,* Vol. 11, pp. 125–134.

Pitts, W. M., 1991b, "Reynolds Number Effects on the Mixing Behavior of Axisymmetric Turbulent Jets," *Experiments in Fluids,* Vol. 11, pp. 135–144.

Richards, C. D., and Pitts, W. M., 1993, "Global Density Effects on the Self-Preservation Behaviour of Turbulent Free Jets," *Journal of Fluid Mechanics,* Vol. 254, pp. 417–435.

Sautet, J. C., and Stepowski, D., 1995, "Dynamic Behavior of Variable-Density, Turbulent jets in their Near Development Fields," *Physics of Fluids,* Vol. 7, pp. 2796–2806.

Schlichting, H., 1979, *Boundary-Layer Theory,* 7th Edition, McGraw-Hill, New York, pp. 596–600.

Stepowski, D., and Sautet, J. C., 1996, "Axial Decay of Unmixedness in Round Turbulent Jets with Variable Density," *IUTAM Symposium on Variable Density Low Speed Turbulent Flows,* July 8–10, Marseille, France.

Thring, M. W., and Newby, M. P., 1953, "Combustion Length of Enclosed Turbulent Jet Flames," *Fourth (Intl) Symposium on Combustion,* The Williams & Wilkins Co., pp. 789–796.

Vradis, G. C., Ötügen, M. V., Kim, S. W., and Kim, D. B., 1993, "Round Incompressible Jets with Asymmetric Initial Velocity Distributions," *AIAA Journal,* Vol. 31, pp. 814–815.

Wu, P.-K., Tseng, L.-K., and Faeth, G. M., 1992, "Primary Breakup in Gas/Liquid Mixing Layers for Turbulent Liquids," *Atomization and Sprays,* Vol. 2, pp. 295–317.

Wu, P.-K., and Faeth, G. M., 1993, "Aerodynamic Effects on Primary Breakup of Turbulent Liquids," *Atomization and Sprays,* Vol. 3, pp. 265–289.

Wu, P.-K., Miranda, R. F., and Faeth, G. M., 1995, "Effects of Initial Flow Conditions on Primary Breakup of Nonturbulent and Turbulent Round Liquid Jets," *Atomization and Sprays,* Vol. 5, pp. 175–196.

Yeh, T. T., and Mattingly, G. E., 1994, "Pipeflow Downstream of a Reducer and its Effects on Flowmeters," *Flow Measurement Instrumentation,* Vol. 5, pp. 181–187.